

Article

Using an Adaptive Neuro-Fuzzy Inference System to Predict Dilution Characteristics of Vertical Buoyant Jets Subjected to Lateral Confinement

Yufeng Zhao ¹, Junshi He ^{1,*}, Xiaohui Yan ²  and Jianwei Liu ²

¹ Faculty of Water Resources Engineering, Shenyang Agricultural University, Shenyang 110065, China; 20141014@stu.syau.edu.cn

² School of Water Resources Engineering, Dalian University of Technology, Dalian 116024, China; yanxh@dlut.edu.cn (X.Y.); jwliu@dlut.edu.cn (J.L.)

* Correspondence: hejunshi@163.com

Abstract: In order to predict the dilution characteristics of vertical buoyant jets constrained by lateral obstructions, we propose a new method based on a commonly used machine learning algorithm: the adaptive neuro-fuzzy inference system (ANFIS). By using experimental data to train and test the ANFIS model, this study shows that it had better performance than commonly used empirical equations for laterally confined jets and another artificial intelligence technique—genetic programming. The RMSE values of the ANFIS-based model were lower, and the R^2 values were higher, compared with those of the empirical equation and genetic programming models. The reduction in RMSE achieved by using ANFIS to replace the empirical equations or genetic programming algorithm exceeded 20%. This research confirms that the ANFIS technique has real potential in the development of effective and accurate models that can be used to estimate the dilution characteristics of a vertical buoyant jet subjected to lateral confinement, providing a new avenue for the prediction of dilution characteristics using artificial intelligence techniques, which can also be utilized for other effluent mixing problems in marine systems.

Keywords: vertical buoyant jet; adaptive neuro-fuzzy inference system; artificial intelligence; dilution characteristics



Citation: Zhao, Y.; He, J.; Yan, X.; Liu, J. Using an Adaptive Neuro-Fuzzy Inference System to Predict Dilution Characteristics of Vertical Buoyant Jets Subjected to Lateral Confinement. *J. Mar. Sci. Eng.* **2022**, *10*, 439. <https://doi.org/10.3390/jmse10030439>

Academic Editor: Bruno Brunone

Received: 26 February 2022

Accepted: 15 March 2022

Published: 18 March 2022

Publisher's Note: MDPI stays neutral with regard to jurisdictional claims in published maps and institutional affiliations.



Copyright: © 2022 by the authors. Licensee MDPI, Basel, Switzerland. This article is an open access article distributed under the terms and conditions of the Creative Commons Attribution (CC BY) license (<https://creativecommons.org/licenses/by/4.0/>).

1. Introduction

Liquid pollutants from coastal domestic waste plants, oil- and gas-related plants, hydropower stations, and other industrial activities are often discharged into the marine system as effluent jets [1,2]. A buoyant jet is a continuous fluid flow containing both momentum and buoyancy fluxes, which can be categorized as a positively or negatively buoyant jet depending on the density difference between the jet and the receiving water body [3,4]. If the density of the jet is lower than that of the surrounding water, the jet is called a positively buoyant jet [5]. Due to the jet's advective and diffusive transport processes, and shear stresses at the interface between the jet and the ambient water, a jet is diluted by the ambient water [6]. Sewage discharges with high pollutant concentrations can potentially seriously harm human health and the coastal environment [7,8], so a better understanding of the mixing characteristics of buoyant jets is very important for the effective design of discharge systems and the accurate assessment of their ecological and environmental impacts.

A jet can be classified as a free or confined jet. If a jet is not close to any obstruction, it is known as a free jet. In practical applications, jets are often affected by boundaries, such as jets within protective riser tubes and those in dredged trenches. These jets are known as confined jets [9]. The dilution and mixing processes of confined jets are typically more complicated than those of simple free jets and plumes; thus, they cannot be predicted using

classical jet and plume theories [10,11]. Turbulent plumes are driven completely by the buoyancy effect, but a buoyant jet is driven by both momentum and buoyancy effects. A free jet can freely spread in, and mix with, the surrounding water; thus, the rapid diffusion of a free jet and the entrainment of ambient water can effectively dilute the effluent of which the jet is composed. However, confinement can restrain free diffusion from a jet and limit the invasion of ambient water into the jet, thereby affecting the dilution of the jet [12]. The existing theories of jets and plumes do not work for confined jets, and new modelling and predictive techniques for this type of jet are needed.

The mixing processes can be studied using experimental, numerical, and artificial intelligence (AI) approaches. Experimental studies have provided comprehensive and reliable datasets for the understanding of the mixing processes of confined jets [12], and have made significant contributions to the estimation of their flow and mixing characteristics. However, in practical applications, the disadvantages of high costs and long implementation times have obstructed the wider usage of experimental observations. Numerical models have also been utilized to study confined jets. Yan and Mohammadian [13] simulated a laterally confined jet using a modified three-dimensional solver in the OpenFOAM platform, and their results demonstrated that the models can satisfactorily predict the mixing properties of buoyant jets subjected to lateral confinement. However, although the costs for numerical studies were lower than experimental approaches, numerical studies require more computational resources. Therefore, there is an urgent need for new predictive tools that are more efficient.

In recent years, with the development of computer science and technology, artificial intelligence (AI) approaches have been adopted to address water environment and marine engineering issues, such as studies of velocity field estimation [14], downscaling of hydrological variables [15], flood forecasting [16–18], streamflow simulations [19], automatic water stage measurements [20], prediction of local scour depth [21], monitoring of oil spills [22], and estimating kinetic parameters [23]. The adaptive neuro-fuzzy inference system (ANFIS) technique is one of the most popular AI techniques, and has been widely employed for various purposes [24,25]. For example, Kisi et al. [24] applied ANFIS techniques for the estimation of sedimentation in rivers. Akpınar et al. [25] studied the performance of an ANFIS model and several parameterization methods for the prediction of wave characteristics using a case study in the Black Sea, and showed that the ANFIS model was more accurate than the parameterization method. Based on an experimental dataset, Mandal et al. [26] established an ANFIS model to predict the degree of damage to breakwaters; results from the ANFIS model were compared with those of artificial neural network (ANN) models, and the results showed that ANFIS was an effective tool to predict the failure degree of non-remodeled slope protection breakwaters. However, the ANFIS algorithm has never been applied to study effluent mixing problems; thus, its suitability in these applications requires further investigation.

In the present study, the ANIFS approach was adopted because it has many merits, such as the capability of capturing the nonlinear structure of a process, adaptation capacity, and rapid learning capability [26]; it can solve nonlinear problems better than traditional methods, such as the moving average model or the autoregressive moving average model. Compared to the other AI techniques, significant advantages of ANFIS are that it has a very rapid learning capability and can be easily accessed using various platforms and software, such as MATLAB. Although AI technologies have significant advantages, few studies have been conducted to predict wastewater dilution characteristics using them. Yan et al. [27–29] utilized the multigene genetic programming (MGGP) algorithm to develop models of jet dilution, but key disadvantages of the MGGP approach are that the scheme is not widely available and the speed of model training is quite slow; furthermore, the approach produces many different models instead of a converged solution, and the solutions significantly change during runs, making it very difficult to obtain stable predictions and repeatable results. Thus, it is important to evaluate whether it is possible to use ANFIS for the prediction of the dilution characteristics of vertical buoyant jets subjected to lateral confinement.

The primary objective of the present study is to propose a new method based on ANFIS to predict the dilution characteristics of vertical buoyant jets hindered by lateral obstruction. An ANFIS-based model was developed, then trained and tested using experimental data. The developed model was used to predict the dilution of a jet at different locations based on the differences in jet and ambient fluid density, the momentum of the jet, and the details of the confinement. Existing empirical equation formulations and a traditional genetic programming approach were used to recalculate the dilution properties, and the performance of the different approaches was compared. To the best of the authors' knowledge, an ANFIS-based model of the dilution of vertical buoyant jets subjected to lateral confinement has never been previously reported.

2. Methodology

2.1. Fundamental Analysis

The main factors affecting a free jet are the discharge volume flux, the buoyancy flux, and the kinematic momentum flux. Using a dimensional analysis, it can be concluded that the dilution of a jet can be estimated based on the port diameter and the densimetric Froude number, which is defined as follows [12,27]:

$$Fr = \frac{u_j}{\sqrt{g'D}} \tag{1}$$

with

$$g' = g \frac{\rho_a - \rho_j}{\rho_a} \tag{2}$$

where u_j = the initial velocity of the jet, g = the gravitational acceleration, ρ_a = the density of the ambient fluid, and ρ_j = the initial density of the jet.

Due to the lateral restriction, the dilution characteristics of a confined jet are more complicated than those of free jets, because the restriction inhibits the transport of the jet and the entrainment of ambient water. The jet concentration can be defined as a function of the densimetric Froude number, the confinement index, and the locations of the cross-sections. Dimensionless forms are commonly utilized in the field; thus, the relevant equations can be effectively applied in practical situations.

Following a dimensional analysis, the dimensionless jet's centerline concentration can be written as $(C_c - C_a)/(C_j - C_a)$, where C_c is the jet's centerline concentration, C_a is the ambient concentration, and C_j is the initial jet's concentration. The dimensionless confinement diameter can be expressed as D_c/D , where D_c is the confinement diameter and D is the port diameter. The dimensionless confinement diameter can be expressed as H_c/D , where H_c is the confinement height. The dimensionless cross-section location can be expressed as Z/D , where Z is the vertical location of the cross-section. The dimensionless confinement diameter and dimensionless confinement height can be manipulated to form the confinement index, which can be expressed as $\beta = (H_c/D)/[(D_c/D) - 1]$.

An empirical formulation that has been widely utilized to calculate the dimensionless jet centerline concentration, and which has been used in this study for comparison to the ANFIS model, can be written as follows [12]:

$$\frac{C_c - C_a}{C_j - C_a} = \frac{(2.594\beta + 1.978)[Z/(DFr)]^{-5/3}}{Fr} \tag{3}$$

2.2. Experimental Data

The experimental data utilized in this study were obtained from Lee and Lee [12], who reported a synthetic dataset for buoyant jets subjected to lateral confinement measured from laboratory experiments. The experimental tank was 1 m long, 1 m wide, and 0.5 m deep, and the water depth was kept at approximately 0.45 m. Water with a higher temperature than the ambient water was vertically issued from the bottom of the water tank into the receiving water from a jet nozzle. Outside the jet nozzle, a tube was installed to simulate confinement.

A laser-induced fluorescence (LIF) system was used to measure the concentration field within the jet.

The experiments investigated the major parameters influencing the jet's mixing properties, and typical ranges for these parameters were tested. Ranges of the densitometric Froude number and confinement index were 3.0–18.7 and 1.47–12.3, respectively. It should be noted that these ranges appear quite narrow, but they cover most of the commonly seen values in nature. Values beyond these ranges are not commonly experienced, so they were not considered in this study. The present study adopted 58 runs, which provided a synthetic dataset with 442 data points. In order to evaluate the performance of the machine learning algorithm, it was necessary to split the experimental dataset into training and testing datasets. In this study, an 80%:20% splitting rule was adopted. Hence, firstly, 80% of the data points were selected to train the model, and then the remaining data were used to evaluate the performance of the model. The raw data were combined and reorganized to obtain the dimensionless parameters, including dimensionless distances, dimensionless concentrations, and densitometric Froude numbers.

2.3. The ANFIS Algorithm

ANFIS is a type of fuzzy reasoning system structure that combines fuzzy logic with neural networks [30]. Fuzzy reasoning systems are widely used in fuzzy control, and neural networks have adaptive learning functions [31]. ANFIS has both of these beneficial characteristics and, hence, has been widely used in fuzzy control, pattern recognition, and other engineering applications [25,32]. ANFIS has the ability to approach any linear or nonlinear function with any required precision, and has a fast convergence speed. Another key merit of ANFIS is that it requires few training samples. The fuzzy inference system (FIS) consists of five modules [30]:

- (1) The rule base of some fuzzy if–then rules;
- (2) A database that defines membership functions of fuzzy sets using fuzzy if–then rules;
- (3) Decision-making units that perform reasoning operations on rules;
- (4) A module that transforms explicit input into a fuzzy interface that matches the value of the language;
- (5) A module that transforms the fuzzy result obtained by reasoning into a clear output deblurring interface.

An adaptive network is a multilayer feedforward network composed of directional links of nodes and connected nodes [33], in which each node performs a specific function (node function) for the incoming signal and a set of parameters related to this node. The structure of an adaptive network contains square nodes with parameters and circular nodes without parameters. The parameter set of an adaptive network is the combination of the parameter set of each adaptive node. Their output depends on the parameters associated with these nodes, and the learning algorithm specifies how to change these parameters.

The model structure of ANFIS is formed by the combination of adaptive network and fuzzy inference system and inherits the interpretable characteristics of the fuzzy inference system and the learning ability of the adaptive network [34]. ANFIS can change the system parameters according to prior knowledge and make the output of the system closer to the real output.

An ANFIS schematic structure diagram is presented in Figure 1, and the example can be interpreted as follows [35]:

- (1) The input x , y is fuzzification in the first layer, for simplicity, assuming that the rule base contains two fuzzy rules [30]: fuzzification membership of a 0~1, usually represented by $U A_i, U B_i$

$$\text{Rule 1: If } x \text{ is } M_1 \text{ and } y \text{ is } N_1, \text{ then } f_1 = p_1x + q_1y + r_1$$

$$\text{Rule 2: If } x \text{ is } M_2 \text{ and } y \text{ is } N_2, \text{ then } f_2 = p_2x + q_2y + r_2$$

- (2) In the second layer, the membership of each feature multiplier yields the trigger strength w_i for each rule. Each node in this layer is a circular node marked as Λ .

$$w_i = \mu A_i(x) \times \mu B_i(y); i = 1; 2:$$

- (3) The third layer normalizes the trigger strength of each rule obtained from the previous layer as the ratio of the sum of the emission intensity of Rule 1 to the firing intensity of all rules, indicating the trigger proportion of the rule in the whole rule library. Each node in this layer is a circular node marked as Γ .

$$w_i^* = w_i / (w_1 + w_2); i = 1; 2:$$

- (4) The results of the fourth inference layer and generally given by a linear combination of input features, and the parameters in that layer will be known as subsequent parameters.

$$w_i^* f_i = w_i^* (p_i x + q_i y + r_i)$$

- (5) The fifth layer's defuzzification yields the exact output, and the final system output is the sum of the results for each rule.

$$F = w_1 \times f_1 / (w_1 + w_2) + w_2 \times f_2 / (w_1 + w_2) = w_1^* \times f_1 + w_2^* \times f_2$$

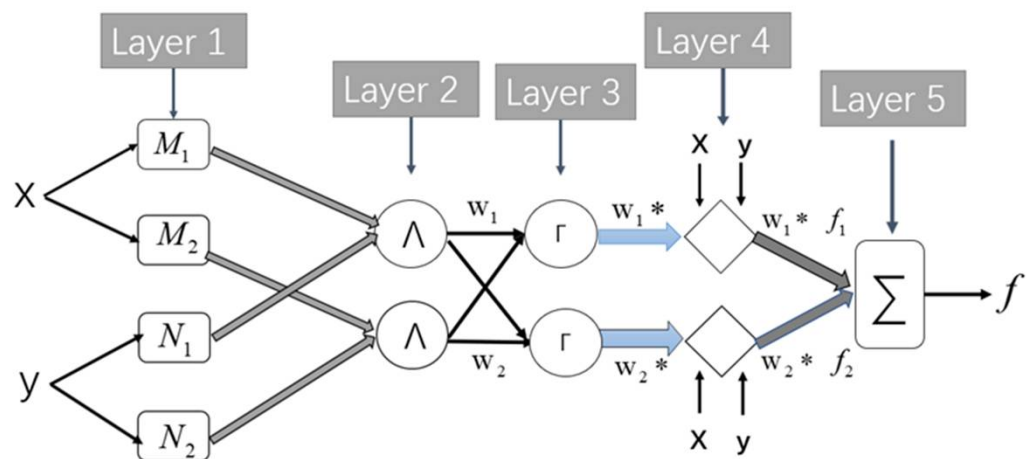


Figure 1. Schematic of an ANFIS structure.

2.4. The ANFIS-Based Model

An ANFIS model of the initial dilution in a transversely constrained, vertical, buoyant jet is established by taking the dimensionless parameters Fr , β , and Z/D as input variables and the dimensionless jet's centerline concentration as the output variable. The input variables (features) are often determined through principal component analyses. However, the present study determined the input variables using theoretical and dimensional analyses. As indicated in Section 2.1, the variables Fr and D can represent the influence of the discharge volume flux, buoyancy flux, and kinematic momentum flux on the mixing processes, and the variable β can describe the influence of the confinement. Therefore, it is believed that the current input variables are the driving factors in the present problem; thus, no additional principal component analyses were performed. The results of the present study demonstrate the performance of the current approach, confirming again that the current selection of the input variables is reasonable.

Data processing was performed in the standard MATLAB environment, and the specific steps were as follows: (1) the available experimental data were divided into a training dataset and a testing dataset; (2) the ANFIS model was trained using the method described above; (3) the developed model was used to calculate the dimensionless jet's

centerline concentration of the training dataset as a function of Fr, β, and Z/D, and the optimal model was selected.

The function “genfis2” available in MATLAB, which generates a Sugeno-type FIS structure, was employed in this study. The present work used subtractive clustering to build an initial network. Subtractive clustering is a fast single algorithm used to estimate the number of clusters and the location of clustering centers in a group of data. Subtractive clustering is used to adaptively adjust the clustering number and clustering center of modeling data in order to determine the number of fuzzy rules and the membership functions of the load model. In this study, the “gaussmf” membership function was utilized as the input membership function, and the linear membership function was employed as the output membership function. The “prod”, “probor”, “prod”, “max”, and “wtaver” were used as the “AND”, “OR”, “Implication”, “Aggregation”, and “Defuzzification” inference methods, respectively. The data network constructed by subtractive clustering was expressed as “in fismat = genfis2 (input_train, output_train, c_i, std)”; the number of training steps was 200. Input_train was a matrix containing the input values of each data point. Output_train was a matrix that contained the output values of each data point. C_i refers to the scope of influence of the clustering centers in each data dimension, which were set as 0.6, 0.4, 0.6, and 0.6, respectively.

Std is an optional matrix of 2 × N, and N is the data (row) dimension. The first row of std indicated that the data value in the data dimension contained the minimum axis range, and the second row recorded whether the data value in the data dimension scaled the maximum axis circumference value of each data dimension. The predicted results were constrained to be positive values. The size of the dataset in this study was comparatively small, which is a very common issue in the field of machine learning, and this weakness can be effectively overcome through careful data splitting or cross-validation approaches. The present study randomly split the data 8 times and then ran the algorithm for each of the data-splitting cases, and found performance to be almost identical. Therefore, the simple train–test split approach, rather than a complicated cross-validation approach (e.g., the k-fold approach), was finally adopted to prevent the overfitting problem and determine the model setup, and this provided convincing conclusions about the performance of the algorithm.

2.5. Performance Indices

The performance of the algorithms was assessed using the mean bias error (MBE), mean absolute error (MAE), root-mean-square error (RMSE) and R-squared (R²) values, given as follows:

$$MBE = \frac{1}{N} \sum_{i=1}^N (x_{calc} - x_{obs}) \tag{4}$$

$$MAE = \frac{1}{N} \sum_{i=1}^N |x_{calc} - x_{obs}| \tag{5}$$

$$RMSE = \sqrt{\frac{1}{N} \sum_{i=1}^N (x_{calc} - x_{obs})^2} \tag{6}$$

$$R^2 = \left\{ \frac{N \sum_{i=1}^N (x_{obs} x_{calc}) - \sum_{i=1}^N (x_{obs}) \sum_{i=1}^N (x_{calc})}{\sqrt{\left[\sum_{i=1}^N (x_{obs}^2) - \left(\sum_{i=1}^N x_{obs} \right)^2 \right] \left[\sum_{i=1}^N (x_{calc}^2) - \left(\sum_{i=1}^N x_{calc} \right)^2 \right]}} \right\}^2 \tag{7}$$

where x_{obs} = observed (actual) data, and x_{calc} = calculated (predicted) data.

3. Results and Discussion

3.1. General Performance

The general performance of the ANFIS model is illustrated in Figure 2, which shows observed and predicted concentration profiles for different scenarios. Concentrations decrease with increasing Z/D as the vertical buoyant jet is diluted along its trajectory due to jet diffusion and ambient water entrainment. When the Fr number is large, the concentration is usually higher, as the buoyancy force becomes less obvious compared to the inertial force at higher Fr numbers. The concentration generally increases with increasing β as the confinement limits diffusion with ambient water, thus reducing dilution. It is obvious that the ANFIS model correctly captures the general characteristics of the observations, indicating that the trained model successfully learned the mechanisms underlying the principal mixing processes.

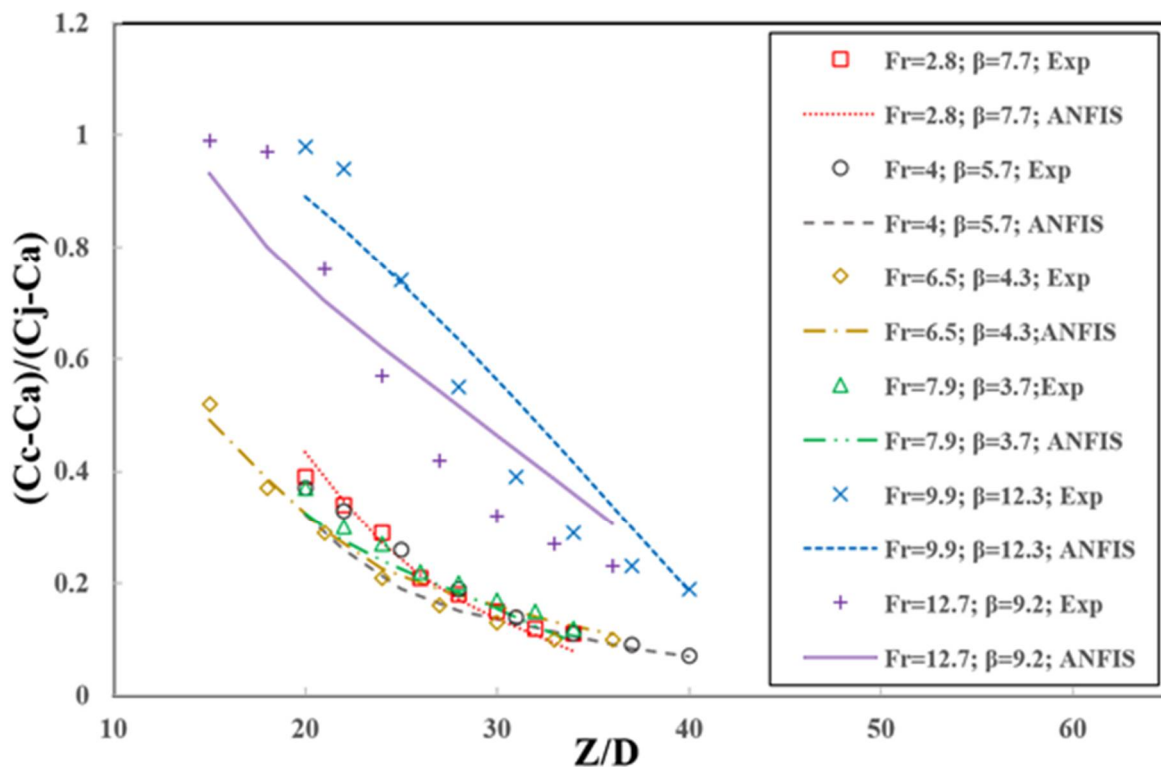


Figure 2. Observed and predicted concentration profiles.

3.2. Comparisons of Observed and Predicted Results

Figure 3 presents a comparison between the experimental and predicted results for all available data points. As can be seen, the ANFIS results closely follow the peaks and troughs of the measured data, indicating that the model can satisfactorily capture the data trend. In this study, predicted values were constrained to be positive, but an upper bound was not considered. The results show that there was only one predicted point exceeding 1, implying that the algorithm can satisfactorily keep the predictions within a reasonable range even without range constraints. Generally, the predicted results matched the experimental data very well. To further evaluate the performance of the model, a scatterplot comparing the training and testing datasets is presented in Figure 3.

To evaluate the predictive capability of the ANFIS technique, the training and testing datasets are separately shown in Figure 4. The testing data points overlap with the training data points very well, indicating that the developed model did not suffer from overfitting. Most of the data points lie close to the 1:1 line, demonstrating the good performance of the ANFIS algorithm for laterally confined jets. A few symbols corresponding to very large

and small values deviate further from the line of agreement. This phenomenon is quite common for AI techniques, which usually perform relatively poorly for extreme data.

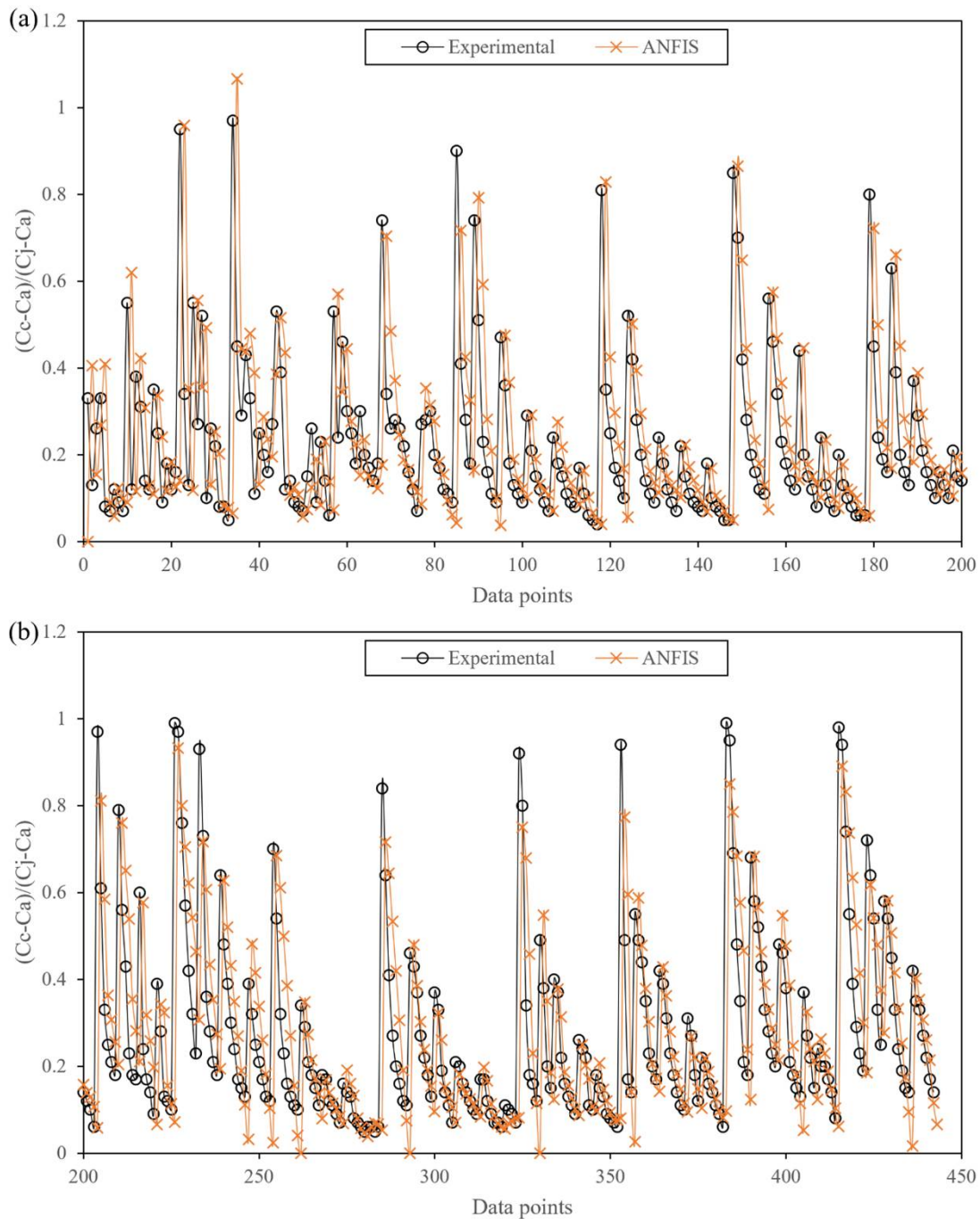


Figure 3. Comparison of the observed and predicted results for all of the data points: (a) data point 0 ~ 200; and (b) data point number >200.

However, overall, the performance of the current algorithm is satisfactory. The performance indices for the ANFIS predictions are summarized in Table 1. The values for the training dataset and testing dataset were close, confirming that the risk of overfitting has been satisfactorily eliminated. Overall, the MBE values were very close to zero, and the value for the entire dataset was 0.002, confirming that the model can satisfactorily control the bias with slight overprediction. The MAE and RMSE values were at magnitudes of ~0.036 and ~0.053, respectively, which were quite low, and the R^2 values were above

0.93, which was quite high, confirming again that the current algorithm can reproduce the experimental data very well.

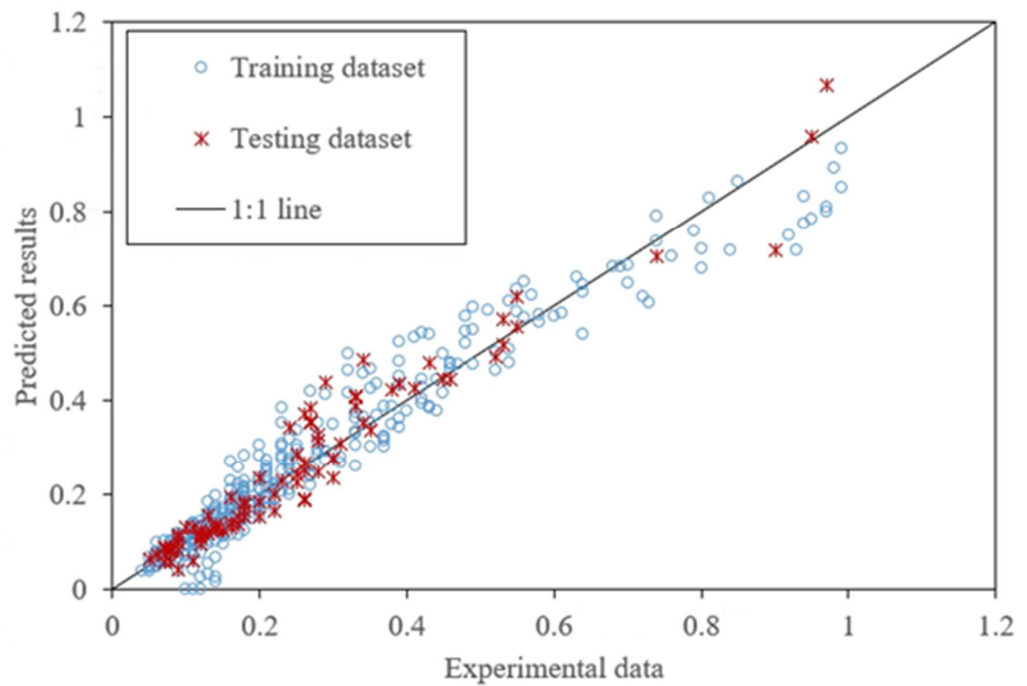


Figure 4. Scatterplot of the measured and predicted data for the training and testing datasets.

Table 1. Performance indices for the ANFIS model predictions.

| Index | Training Dataset | Testing Dataset | Entire Dataset |
|----------------|------------------|-----------------|----------------|
| MBE | 0.000 | 0.007 | 0.002 |
| MAE | 0.037 | 0.034 | 0.036 |
| RMSE | 0.054 | 0.049 | 0.053 |
| R ² | 0.934 | 0.938 | 0.934 |

3.3. Comparison with the Empirical Equations and Genetic Programming Methods

Dimensionless jet concentrations were also predicted using existing empirical equations, as well as using the genetic programming algorithm. All predictions are compared in Figure 5. The empirical equation used is described in Equation (3).

The genetic programming analyses were conducted primarily using the MATLAB code GPTIPS2 [36], which was adapted to solve the problem in this study. The following parameters, determined by cross-validations, were utilized: population size = 250, maximum generations = 150, tournament size = 20, probability of Pareto tournament = 0.3, maximum depth of the chromosome tree = 5, elite fraction = 0.3, crossover probability = 0.84, and mutation probabilities = 0.14. The genetic programming approach can provide explicit equations, and the best performing equation for this case can be expressed as $(C_c - C_a)/(C_j - C_a) = [29.1\beta(Fr + Z/D - 8.6)]/(Z/D)^3 + 0.00997$.

As can be seen in Figure 5, the results obtained by the three methods were close, indicating that all of these methods can produce acceptable predictions. The performance indices for three prediction methods are summarized in Table 2. The performance of the empirical equation and that of the genetic programming algorithm were almost identical, and their RMSE values exceeded 0.065 while their R² values were below 0.9. However, the ANFIS model provided the best predictions and, in terms of RMSE, reduced the error index by more than 20%.

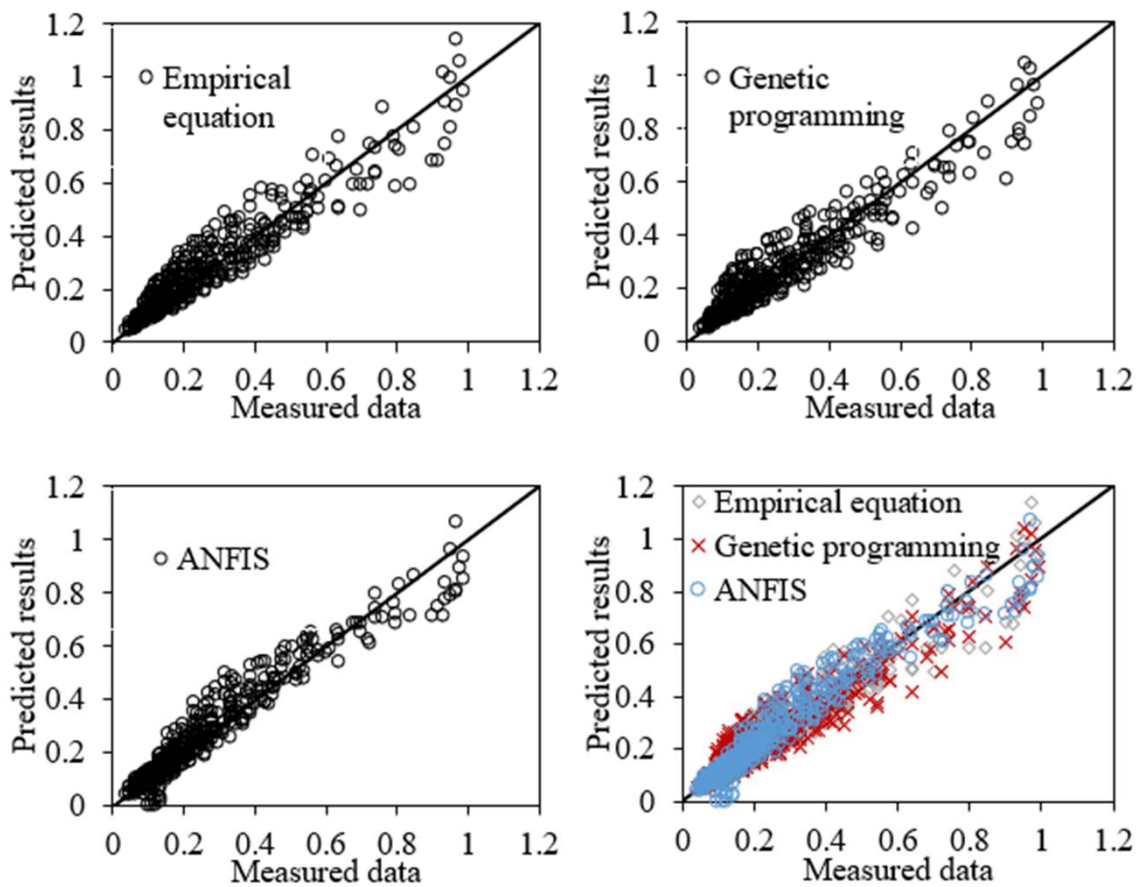


Figure 5. Comparison of observations with predictions obtained by three different methods: empirical equations, genetic programming, and the ANFIS model.

Table 2. Performance indices for the predictions obtained by three different methods: empirical equations, genetic programming, and the ANFIS model.

| Index | Empirical Equation | Genetic Programming | ANFIS |
|----------------|--------------------|---------------------|-------|
| RMSE | 0.068 | 0.067 | 0.053 |
| R ² | 0.895 | 0.894 | 0.934 |

3.4. Novelty and Limitations

To the best of the authors’ knowledge, the use of an adaptive neuro-fuzzy inference system for predicting mixing processes has not been previously reported. A major contribution of this study is that it demonstrates that the ANFIS algorithm can reasonably predict the dilution characteristics of vertical buoyant jets subjected to lateral confinement. The proposed approach can facilitate accurate estimation of the mixing characteristics of vertical buoyant jets subjected to lateral confinement because it can provide rapid predictions of the key mixing features for arbitrary densitometric Froude numbers, port diameters, and confinement indices. It is meaningful to develop such AI-based models for predicting the dilution characteristics of effluents, because experimental and numerical methods are typically more expensive and time consuming, whereas AI models can provide cost-effective predictions in seconds.

Compared to the empirical formulation, which was derived using a traditional regression approach, the present approach is more accurate, and can be further improved when more data are available. The current ANFIS predictions performed better than the genetic programming algorithm, but the major advantage of ANFIS over genetic programming techniques is that ANFIS is a readily available AI algorithm and can be easily accessed in

many programs. It should be acknowledged that the genetic programming algorithm can provide explicit equations while ANFIS cannot, but the ANFIS algorithm can be readily utilized, is fast to run, and its predictions are generally more stable, so it can be seen as a valuable complementary approach. As the genetic programming algorithm can provide explicit equations, prediction confidence analysis can be performed using the symmetric confidence interval approach. However, ANFIS cannot provide explicit equations, so the same analysis cannot be conducted. The primary objective of this study was to investigate the ANFIS approach for predicting confined vertical buoyant jets and demonstrate its suitability. In future studies, the uncertainty of the algorithm should be quantified using suitable approaches to further assess the performance of the algorithm. A limitation of the present study is that the model was only trained and validated against well-controlled experimental data. This demonstrates that the algorithm can satisfactorily learn the underlying mechanism of the phenomenon, but its performance for practical applications should also be further evaluated in future studies.

4. Summary and Conclusions

The present study proposes a new approach based on ANFIS for the estimation of the initial dilution of laterally confined jets. The model can produce fast predictions of the jets' centerline concentration based on a confinement index and the densitometric Froude number. The predicted results were compared against experimental data, and the results showed that the ANFIS model can satisfactorily reproduce the data. The existing empirical equations method and the traditional genetic programming method were also utilized to analyze the same problem, and the results confirmed that the ANFIS algorithm can outperform these other methods. The performance of the empirical equations and that of the genetic programming algorithm were almost identical. In terms of RMSE, the ANFIS algorithm reduced the associated errors by more than 20%. The principal benefit of using an ANFIS-based model to predict effluent mixing problems is that the algorithm is readily available and can be easily accessed. The proposed approach also has many other merits, such as the capability of capturing the nonlinear structure of a process, adaptation capacity, and rapid learning capability. The results of this study confirm that the proposed approach based on ANFIS is promising for estimating effluent mixing phenomena, and can facilitate accurate estimation of the mixing characteristics of vertical buoyant jets subjected to lateral confinement; it can also provide rapid predictions of the key mixing features for arbitrary densitometric Froude number, port diameter, and confinement index. Future studies should be conducted in order to further quantify the uncertainty of the approach and evaluate its performance in practical applications.

Author Contributions: The authors equally contributed to the present work. All authors have read and agreed to the published version of the manuscript.

Funding: This research was funded by the Fundamental Research Funds for the Central Universities (China; DUT20RC(3)096).

Institutional Review Board Statement: Not applicable.

Informed Consent Statement: Not applicable.

Acknowledgments: This research was funded by the Fundamental Research Funds for the Central Universities (China; DUT20RC(3)096). We would like thank the editors and reviewers for their careful reading of our manuscript, and their insightful comments and suggestions.

Conflicts of Interest: The authors declare no conflict of interest.

References

1. Chow, A.C.; Shrivastava, I.; Adams, E.E.; Al-Rabaie, F.; Al-Anzi, B. Unconfined dense plunging jets used for brine disposal from desalination plants. *Processes* **2020**, *8*, 696. [[CrossRef](#)]
2. Hussein, H.; Capp, S.; George, W. Velocity measurements in a high-Reynolds-number, momentum-conserving, axisymmetric, turbulent jet. *J. Fluid Mech.* **1994**, *258*, 31–75. [[CrossRef](#)]

3. Mohammadian, A.; Gildeh, H.K.; Nistor, I. CFD modeling of effluent discharges: A review of past numerical studies. *Water* **2020**, *12*, 856. [\[CrossRef\]](#)
4. Kheirkhah Gildeh, H.; Mohammadian, A.; Nistor, I. Inclined dense effluent discharge modelling in shallow waters. *Environ. Fluid Mech.* **2021**, *21*, 955–987. [\[CrossRef\]](#)
5. Ardalan, H.; Vafaei, F. CFD and Experimental Study of 45° Inclined Thermal-Saline Reversible Buoyant Jets in Stationary Ambient. *Environ. Process* **2019**, *6*, 219–239. [\[CrossRef\]](#)
6. Wu, J.Y.; Lv, R.R.; Huang, Y.Y.; Yang, G. Flow structure transition and hysteresis of turbulent mixed convection induced by a transverse buoyant jet. *Int. J. Heat Mass Transf.* **2021**, *177*, 121310. [\[CrossRef\]](#)
7. Khosravi, M.; Javan, M. Three-dimensional flow structure and mixing of the side thermal buoyant jet discharge in cross-flow. *Acta Mech.* **2020**, *231*, 3729–3753. [\[CrossRef\]](#)
8. Xu, Z.; Otoo, E.; Chen, Y.; Ding, H. 2D PIV measurement of twin buoyant jets in wavy cross-flow environment. *Water* **2019**, *11*, 399. [\[CrossRef\]](#)
9. Turner, J.S. Turbulent entrainment: The development of the entrainment assumption, and its application to geophysical flows. *J. Fluid Mech.* **1986**, *173*, 431–471. [\[CrossRef\]](#)
10. Morton, B.R.; Taylor, G.I.; Turner, J.S. Turbulent gravitational convection from maintained and instantaneous sources. *Proc. R. Soc. Lond. Ser. A. Math. Phys. Sci.* **1956**, *234*, 1–23.
11. Manins, P.C. Turbulent buoyant convection from a source in a confined region. *J. Fluid Mech.* **1979**, *91*, 765–781. [\[CrossRef\]](#)
12. Lee, A.W.T.; Lee, J.H.W. Effect of lateral confinement on initial dilution of vertical round buoyant jet. *J. Hydraul. Eng.* **1998**, *124*, 263–279. [\[CrossRef\]](#)
13. Yan, X.; Mohammadian, A. Numerical Modeling of Vertical Buoyant Jets Subjected to Lateral Confinement. *J. Hydraul. Eng.* **2017**, *143*, 04017016. [\[CrossRef\]](#)
14. Kreyenberg, P.J.; Bauser, H.H.; Roth, K. Velocity field estimation on density-driven solute transport with a convolutional neural network. *Water Resour. Res.* **2019**, *55*, 7275–7293. [\[CrossRef\]](#)
15. Wang, F.; Tian, D.; Lowe, L.; Kalin, L.; Lehrter, J. Deep learning for daily precipitation and temperature downscaling. *Water Resour. Res.* **2021**, *57*, e2020WR029308. [\[CrossRef\]](#)
16. Kabir, S.R.; Patidar, S.; Xia, X.; Liang, Q.; Pender, G. A deep convolutional neural network model for rapid prediction of fluvial flood inundation. *J. Hydrol.* **2020**, *590*, 125481. [\[CrossRef\]](#)
17. Lei, X.; Chen, W.; Panahi, M.; Falah, F.; Bian, H. Urban flood modeling using deep-learning approaches in Seoul, South Korea. *J. Hydrol.* **2021**, *601*, 126684. [\[CrossRef\]](#)
18. Wang, Y.; Fang, Z.; Hong, H.; Peng, L. Flood susceptibility mapping using convolutional neural network frameworks. *J. Hydrol.* **2020**, *582*, 124482. [\[CrossRef\]](#)
19. Yang, S.; Yang, D.; Chen, J.; Santisirisomboon, J.; Zhao, B. A physical process and machine learning combined hydrological model for daily streamflow simulations of large watersheds with limited observation data. *J. Hydrol.* **2020**, *590*, 125206. [\[CrossRef\]](#)
20. Eltner, A.; Bressan, P.O.; Akiyama, T.; Goncalves, W.N.; Marcato Junior, J. Using deep learning for automatic water stage measurements. *Water Resour. Res.* **2021**, *57*, e2020WR027608. [\[CrossRef\]](#)
21. Bashiri, H.; Sharifi, E.; Singh, V.P. Prediction of local scour depth downstream of sluice gates using harmony search algorithm and artificial neural networks. *J. Irrig. Drain. Eng.* **2018**, *144*, 06018002. [\[CrossRef\]](#)
22. Moroni, D.; Pieri, G.; Tampucci, M. Environmental Decision Support Systems for Monitoring Small Scale Oil Spills: Existing Solutions, Best Practices and Current Challenges. *J. Mar. Sci. Eng.* **2019**, *7*, 19. [\[CrossRef\]](#)
23. Dolan, K.D.; Yang, L.; Trampel, C.P. Nonlinear regression technique to estimate kinetic parameters and confidence intervals in unsteady-state conduction-heated foods. *J. Food Eng.* **2007**, *80*, 581–593. [\[CrossRef\]](#)
24. Kisi, O. Suspended sediment estimation using neuro-fuzzy and neural network approaches. *Hydrol. Sci. J.* **2005**, *50*, 696. [\[CrossRef\]](#)
25. Akpınar, A.; Özger, M.; Kömürçü, M.I. Prediction of wave parameters by using fuzzy inference system and the parametric models along the south coasts of the Black Sea. *J. Mar. Sci. Technol.* **2014**, *19*, 1–14. [\[CrossRef\]](#)
26. Mandal, S.; Rao, S.; Harish, N. Damage level prediction of non-reshaped berm breakwater using ANN, SVM and ANFIS models. *Int. J. Nav. Archit. Ocean. Eng.* **2012**, *4*, 112–122. [\[CrossRef\]](#)
27. Yan, X.; Mohammadian, A. Evolutionary modeling of inclined dense jets discharged from multiport diffusers. *J. Coast. Res.* **2019**, *36*, 362–371. [\[CrossRef\]](#)
28. Yan, X.; Mohammadian, A. Multigene Genetic-Programming-Based Models for Initial Dilution of Laterally Confined Vertical Buoyant Jets. *J. Mar. Sci. Eng.* **2019**, *7*, 246. [\[CrossRef\]](#)
29. Yan, X.; Mohammadian, A. Evolutionary prediction of the trajectory of a rosette momentum jet group in flowing currents. *J. Coast. Res.* **2020**, *36*, 1059–1067. [\[CrossRef\]](#)
30. Jang, J.-S.R. ANFIS: Adaptive-network-based fuzzy inference system. *IEEE Trans. Syst. Man Cybern.* **1993**, *23*, 665–685. [\[CrossRef\]](#)
31. Tatikonda, R.C.; Battula, V.P.; Kumar, V. Control of inverted pendulum using adaptive neuro fuzzy inference structure (ANFIS). In Proceedings of the 2010 IEEE International Symposium on Circuits and Systems, Paris, France, 30 May–2 June 2010.
32. Xue, X.; Yang, X. Application of the adaptive neuro-fuzzy inference system for prediction of soil liquefaction. *Nat. Hazards* **2013**, *67*, 901–917. [\[CrossRef\]](#)
33. Sayama, H.; Pestov, I.; Schmidt, J.; Bush, B.J.; Wong, C.; Yamanoi, J.; Gross, T. Modeling complex systems with adaptive networks. *Comput. Math. Appl.* **2013**, *65*, 1645–1664. [\[CrossRef\]](#)

34. Yadollahi, M.M.; Benli, A.; Demirboga, R. Application of adaptive neuro-fuzzy technique and regression models to predict the compressive strength of geopolymer composites. *Neural Comput. Appl.* **2017**, *28*, 1453–1461. [[CrossRef](#)]
35. Hosseini, M.S.; Moradi, M.H. Adaptive fuzzy-sift rule-based registration for 3D cardiac motion estimation. *Appl. Intell.* **2022**, *52*, 1615–1629. [[CrossRef](#)]
36. Searson, D.P. GPTIPS 2: An open-source software platform for symbolic data mining. In *Handbook of Genetic Programming Applications*; Springer: Cham, Switzerland, 2015; pp. 551–573.